



Aldol condensation products during photocatalytic oxidation of ethanol in a photoelectrochemical cell

Paraskevi Panagiotopoulou^a, Maria Antoniadou^b, Dimitris I. Kondarides^{a,*}, Panagiotis Lianos^b

^a Department of Chemical Engineering, University of Patras, GR-26504 Patras, Greece

^b Engineering Science Department, University of Patras, GR-26504 Patras, Greece

ARTICLE INFO

Article history:

Received 4 June 2010

Received in revised form 13 July 2010

Accepted 16 July 2010

Available online 22 July 2010

Keywords:

Aldol condensation

Photocatalytic oxidation

PhotoFuelCell

Ethanol

Titanium dioxide

ABSTRACT

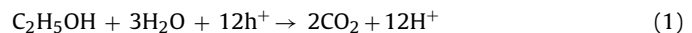
Electric current was produced in a photoelectrochemical cell during photocatalytic oxidation of ethanol, which was used as a representative organic compound present in wastewater from biomass processing industries. Thus, the cell behaved as a PhotoFuelCell that consumed waste material to produce electricity. The cell consisted of two compartments separated by a silica frit. The anode electrode was a Fluorine-doped Tin Oxide transparent electrode bearing nanocrystalline titania Degussa P25, applied as a paste and calcined at 550 °C. The cathode electrode was a carbon-cloth bearing Pt/Carbon-Black catalyst. The electrolyte was 1.0 M NaOH. When 20%v. ethanol was added in the anode compartment, the cell gave 0.75 mA/cm² short-circuit current density (calculated over 12 cm² electrode area) and 1.1 V open-circuit voltage. The anode compartment of the cell was operated under three different conditions: (1) under continuous air flow, i.e. oxygen-rich conditions; (2) under Ar flow, i.e. anaerobic conditions; and (3) exposed to ambient air but without any gas flow through the cell, i.e. oxygen-deficient, mass transfer-limited conditions. In the latter two cases, the oxidation of ethanol and its photo-oxidation products was incomplete and resulted in aldol condensation reactions that produced various aldehydes, some of them of high molecular weight and insoluble. It was concluded that in order to avoid such reactions, which impede mineralization process, measures should be taken for continuous oxygen supply and for optimal combination of the quantity of the photocatalyst and the concentration of the photodegradable substance. Thus only 1%v. ethanol can give 75% of the maximum current obtained in the presence of large ethanol concentration.

© 2010 Elsevier B.V. All rights reserved.

1. Introduction

Photocatalytic oxidation of organic substances in a photoelectrochemical cell can be used as a source of electricity, as has been shown in previous studies [1–8]. Thus, a photoelectrochemical cell can act as a PhotoFuelCell (PFC) [1–3,8] that consumes organic wastes to produce electricity. Such cells provide a double environmental benefit, that is, renewable energy can be produced with consumption of waste organic materials, byproducts of biomass processing industries and pollutants. The main component of a PFC is a semiconductor photoanode, typically nanocrystalline titania (nc-TiO₂), where the photocatalytic oxidation is carried out. A standard configuration of a PFC is schematically shown in Fig. 1. The cell consists of two compartments divided by an ion transfer membrane. Various materials can be employed for this purpose, including Nafion membrane, which mainly allows transfer of protons but is also permeable to alkaline cations. In the present work

a silica frit was used, which makes no distinction in the transfer of both ionic and cationic species. The cathode was made of a catalytic material based on a carbon cloth bearing commercial Pt/carbon-black catalyst. NaOH electrolyte was used in both compartments but the anode compartment also contained the fuel. Ethanol was used as a model fuel in the present work for reasons of simplicity but many other substances could be employed as well. The main ionic species diffusing through the frit is expected to be OH[–] ions. Indeed, excitation of the semiconductor photocatalyst by light absorption leads to generation of electrons and holes. Holes drive the oxidation reactions, which, in the case of ethanol, are represented by the following overall reaction scheme (cf. Refs. [9,10]):



In the presence of a strongly basic environment, as is the present case, hydrogen ions are consumed producing water:



Thus (1) and (2) are fused into the following reaction:



* Corresponding author. Tel.: +30 2610 969527; fax: +30 2610 991527.

E-mail address: dimi@chemeng.upatras.gr (D.I. Kondarides).

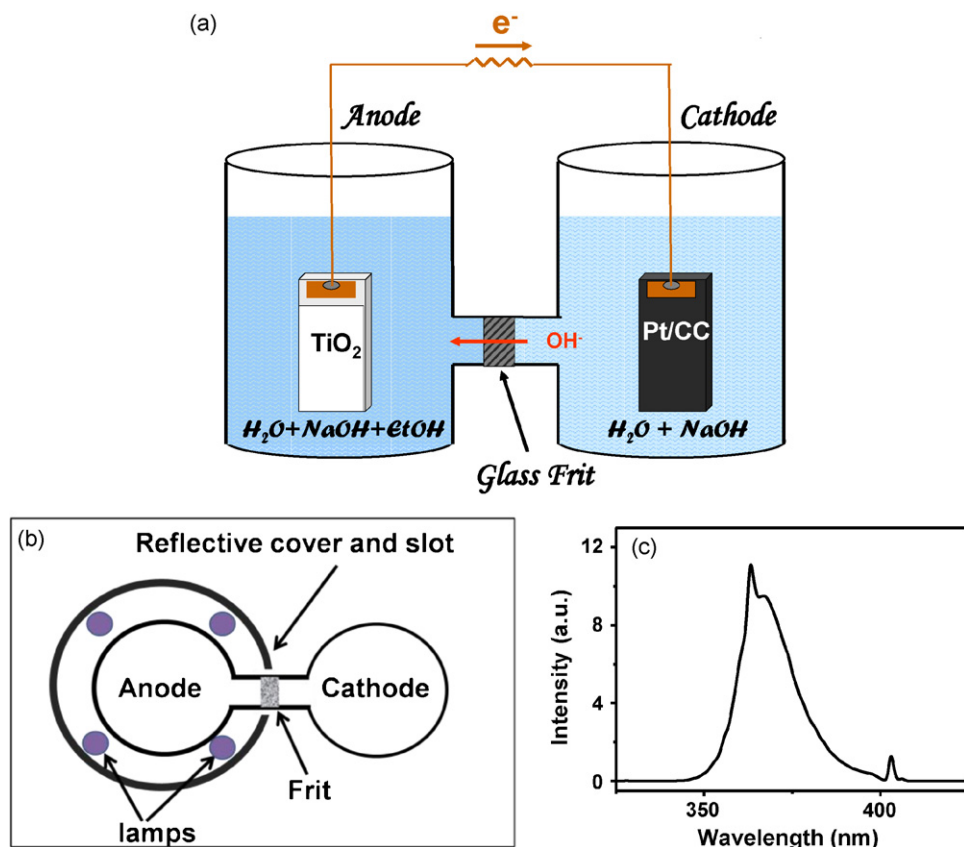


Fig. 1. (a) Schematic representation of the reactor. The anode compartment contained 150 ml of an aqueous solution of ethanol at various concentrations and 1 M NaOH. The cathode compartment contained the same electrolyte as the anode compartment but without alcohol. Diffusion of OH⁻ ions is expected from the cathode to the anode compartment through the glass frit; (b) horizontal cross section showing placement of anode compartment within the cavity supporting the four Black Light tubes; (c) emission spectrum of the light source (Black Light).

The fate of photogenerated electrons depends on the applied conditions. Electrons flow through the external circuit towards the cathode where under aerated conditions in the cathode compartment, that is, in the presence of oxygen, they drive the O₂-reduction reaction:



Thus OH⁻ ions are regenerated, feeding the system in a cyclic manner. In other words, hydroxyl ions are consumed during oxidation and they are regenerated during reduction. Since OH⁻ are regenerated in the cathode compartment and since the NaOH concentration is the same in both compartments, it is expected that during cell operation there exists a continuous flow of OH⁻ from the cathode to the anode compartment as shown in Fig. 1a.

Reactions (1)–(3) can be carried out in the absence of oxygen. In that case, they describe a photocatalytic alcohol reforming reaction, in which the oxidant is water. In the presence of oxygen, which is a much more efficient oxidant than water, these reactions are not excluded but the dominant reaction should be photocatalytic alcohol combustion, as described by the following overall reaction (5) and also discussed in Section 4.3:



In the course of studying such cells as well as in previous studies of chemically biased cells employing Nafion membrane [6–8], we found that the color of the solution in the anode compartment progressively became increasingly yellow. This is contrary to what is usually expected in a photo-oxidation process, where complete mineralization is the set target. Obviously, new species are formed in the solution, which cannot be always consumed by

the photocatalytic process. Preliminary studies presented in a previous publication using a chemically biased cell [11], revealed the occurrence of aldol condensation reactions. It seems, however, that such processes do take place under more general conditions. Thus, the present work studies this case more extensively and proposes conditions of PFC functioning without interference from counterproductive processes.

2. Experimental

2.1. Materials

Unless otherwise indicated, reagents were obtained from Aldrich and were used as received. The nanocrystalline titania was commercial Degussa P25. Millipore water was used in all experiments. SnO₂:F transparent conductive electrodes (FTO, Resistance 8 Ω/square) were purchased from Pilkington, USA. Carbon Cloth, 20% wet proofing and Pt/Carbon Black electrocatalyst (30% on Vulcan XC72) were purchased from BASF Fuel Cell, Inc., USA. Carbon Black (Vulcan XC72R) was a gift from CABOT Corporation.

2.2. Preparation of the anode

Anode electrodes were based on commercial titania. Degussa P25 was applied on FTO electrodes using a home-made paste, which was prepared according to the recipe given in Ref. [12]. Two layers of titania were applied giving a uniform film of about 8–10 μm thick. An image of such a film can be seen in Ref. [13]. The film was calcined at 550 °C. The geometric surface of each titania film was 3 × 4 = 12 cm². A picture of a similar electrode can be seen in Ref.

[14]. Electric contact was made by using an adhesive copper ribbon and a copper wire soldered on the copper ribbon.

2.3. Preparation of the cathode

Special care was taken for the construction of the cathode electrode, in order to increase its efficiency. Cathode was made of carbon cloth with deposited Carbon Black and Pt as described in a previous publication [8]. An amount of 0.246 g of Carbon Black was mixed with 8 ml of distilled water by vigorous mixing in a mixer (about 2400 r.p.m.) until it became a viscous paste. This paste was further mixed with 0.088 ml polytetrafluoroethylene (Aldrich, Teflon 60 wt.% dispersion in water) and then applied on a carbon cloth cut in the necessary dimensions. This has been achieved by first spreading the paste with a spatula, preheating at 80 °C and finally heating in an oven at 340 °C. Subsequently, the catalytic layer was prepared as follows: 1 g of Pt/Carbon Black electrocatalyst (30% on Vulcan XC72) was mixed with 8 g of Nafion perfluorinated resin (5 wt.% solution in lower aliphatic alcohols and water, Aldrich) and 15 g of a solution made of 7.5 g H₂O and 7.5 g isopropanol. The mixture was ultrasonically homogenized and then applied on the previously prepared carbon cloth bearing Carbon Black. Then, the electrode was heated at 80 °C for 30 min and the procedure was repeated as many times as necessary to load about 0.5 mg of Pt/cm². The thus prepared Pt/carbon-cloth (Pt/CC) electrode was ready for use. Its size was similar to that of the anode electrode, i.e. 3 × 4 = 12 cm².

2.4. Description of the reactor

The reactor was made of pyrex glass of cylindrical shape (55 mm internal diameter) and it had an H shape (Fig. 1a). The two compartments were separated by a silica frit (ROBU, Germany, porosity SGQ 5, diameter 25 mm, thickness 2 mm). Both compartments could be tightly capped with pyrex fittings having provisions for electrode connections and gas inlet–outlet. The cathode compartment was in all cases exposed to the ambient. The anode compartment run under three different conditions: inert gas (Ar) flow; air flow; and still solution exposed to the ambient. The outlet of the anode compartment was connected to a nondispersive infrared (NDIR) analyzer (Binos) for on-line measurement of CO₂ concentration in the gas-phase. Each compartment could carry about 150 ml of electrolyte. The electrolyte was an aqueous solution of 1.0 M NaOH. UVA excitation of titania was made by using 4 Black Light fluorescent tubes (Fig. 1b), peaking around 363 nm (Fig. 1c). The tubes, each of 4 W nominal power, were placed around the anode compartment and they were covered by a cylindrical protecting-reflecting cover, having a slot that allowed the cathode compartment to be placed outside the lamp system in the dark (cf. Fig. 1b). This reactor and excitation source configuration was very convenient for the present application, since it was not sensitive to sample direction or position in the cavity. The total radiation intensity incident on the sample was estimated to be around 3.5 mW/cm².

2.5. Measuring procedures for UV/vis and GC/MS analysis

The alkaline ethanol–water solution was exposed to UVA light at $t = 0$ and left under irradiation for 96 h in order to study photoinduced reactions of ethanol. During this period, the cell operated under short-circuit conditions. Illumination of the photocatalyst was then interrupted and the system was left in the dark for another 27 h in order to study the extent of reactions that may take place in the absence of light. During this time period and at regular time intervals, samples (4 ml) were taken from the solution for identification and quantification of reaction products present in the liquid phase with the use of UV/vis and GC/MS techniques. The collected samples were immediately analyzed with UV/vis spectrophotom-

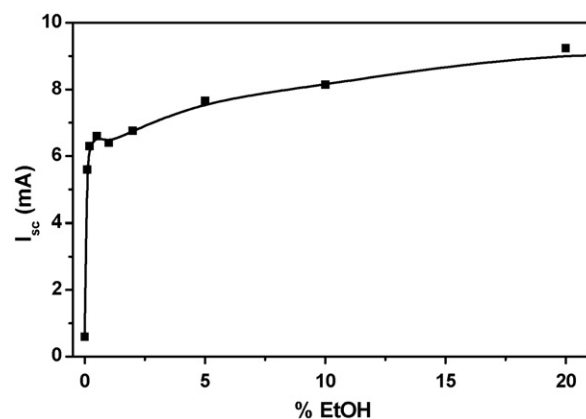


Fig. 2. Variation of the short-circuit current as a function of ethanol volume percent. The electrolyte contained 1 M NaOH. Measurements were made with fresh samples.

etry (Hitachi, model U 2001) using 10 mm quartz cuvettes and the initial (transparent) solution as reference. After this measurement, the largest part of the sample was returned to the reactor vessel whereas 1 ml of it was filtered with the use of syringe filters and stored in sealed vials in a refrigerator for subsequent GC/MS analysis. Filtering of the samples before admission to the GC/MS system was necessary for the protection of the injector and column, because certain samples contained small particles produced by oligomerization of reaction products (see below).

2.6. Apparatus

Electrochemical measurements were carried out with an AutoLab potentiostat PGSTAT128N. Radiation intensity was measured with a PMA 2100 Radiant Power meter (Solar Light Co), calibrated for the Near UV spectral range. GC (Hewlett Packard 6890) was equipped with an HP-Innowax capillary column (30 m × 0.25 mm × 0.25 μm film thickness) and was interfaced directly to the MS (HP 5973) used as detector. The GC analysis was performed with the use of 1 μL of pre-filtered samples in a temperature-programmed mode with an initial temperature of 35 °C held for 5 min, then ramped at 5 °C/min up to 150 °C and finally ramped at 20 °C/min up to 250 °C and held at that temperature for 10 min. Identification of the GC/MS spectral features has been achieved with the use of a build-in library. Quantification of the detected compounds was made with the use of self-prepared aqueous solutions of ethanol (20% v.) containing known amounts of acetaldehyde, crotonaldehyde, hexadienal and acetone.

3. Results

3.1. Current–voltage characteristics of the cell

The current–voltage characteristics of the cell were measured with fresh electrolyte and fuel, using various concentrations of added ethanol. The short-circuit current of the cell increased with EtOH concentration. As seen in Fig. 2, it increased sharply at small EtOH concentrations but then it reached saturation. At 20% v. EtOH and under the present experimental conditions, the short-circuit current was 9.0 mA (0.75 mA/cm²) and the open-circuit voltage was 1.1 V. The present results were obtained with aerated electrolyte in the cathode compartment. In the absence of oxygen, both voltage and current dramatically dropped. Therefore, no measurements were made under anaerobic conditions in the cathode compartment. The evolution of the current in the course of time can be seen in Fig. 3. In all cases current decreased. This decrease of current may be due to several different reasons but we believe that

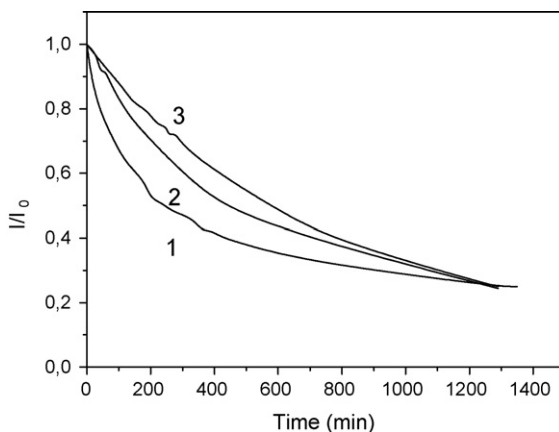


Fig. 3. Variation of the short-circuit current as a function of irradiation time in a reactor containing 20% v/v ethanol and 1.0 M NaOH: (1) measurement was made under continuous flow of air through the solution; (2) no flow of any gas. Solution was still but exposed to ambient air; (3) continuous flow of Ar. Current was normalized to its initial value (at $t=0$), i.e., expressed in all cases as I/I_0 , for comparison reasons.

the most important one is the partial deactivation of photocatalytically active sites on titania. Such situations are very frequently observed in photocatalysis, and can be attributed to formation of stable reaction intermediates that cover the photocatalyst surface, to “poisoning” of active sites by species present in the electrolyte solution, to partial etching of the photocatalyst due to the strongly alkaline environment, etc. This conclusion is supported by the fact that when the anode electrode was replaced by an unused similar electrode, the current recuperated its original value. The fastest current decrease was observed in the case when air was pumped through the solution, while under Ar flow the decrease of current was the slowest. An intermediate situation was established when the solution stayed still but was exposed to the ambient. The fastest decrease of current in the case of air flow is in accordance with the above assumption of deactivation of photocatalytic active sites. Thus, under anaerobic conditions, deactivation of these sites is much slower. The original absolute values of the current were 6.6 mA in the case of air-flow through the anode, 9 mA without any gas flow and 10.5 mA in the case of Ar flow. These values again describe the importance of the presence of oxygen. Thus in its presence, photogenerated electrons are partly scavenged by O_2 and this affects the number of electrons flowing through the external circuit.

After several hours of cell functioning, the solution obtained a yellow coloration. The color was very deep in the case of Ar flow but it was hardly distinguishable in the case of air flow. It is obvious that when air (i.e., oxygen) flows through the solution in the anode compartment then oxidation of the fuel is faster. For this reason, subsequent experiments were carried out using an intermediate situation, i.e., no gas flow through the anode compartment. The following data have been obtained by continuously running the reactor for a few days under short-circuit conditions, that is, anode and cathode were externally connected with a wire of practically zero resistance.

3.2. GC/MS analysis

The main reaction products detected in solution by GC/MS, following irradiation of the anode compartment, were acetaldehyde ($t_R = 1.9$ min), crotonaldehyde ($t_R = 7.3$ min), 2,4-hexadienal ($t_R = 18.5$ min), and acetone ($t_R = 2.5$ min). Results obtained are summarized in Fig. 4, where the concentrations of the detected reaction products are plotted as a function of time, i.e., 96 h under irradiation followed by 27 h under dark conditions. It is observed that immediately after illumination, acetaldehyde appeared in the li-

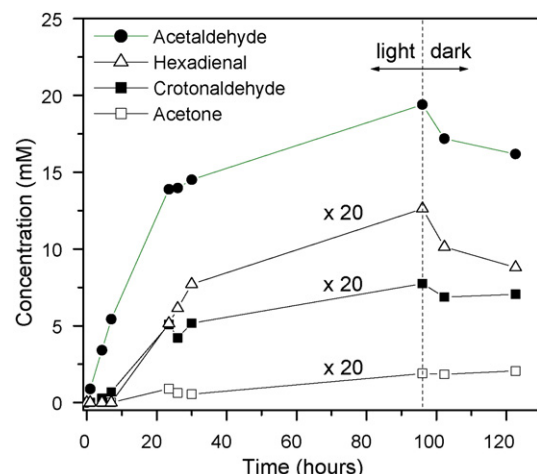


Fig. 4. Variation of the concentration of species in the anode compartment during irradiation and in the dark, as detected by GC-MS.

uid phase and its concentration increased with illumination time. Prolonged exposure to light resulted in the production of measurable amounts of crotonaldehyde after ca 4 h, whereas longer illumination times were required for the detection of hexadienal and acetone (Fig. 4). The concentrations of crotonaldehyde, hexadienal and acetone, which were significantly lower, compared to that of acetaldehyde, progressively increased with illumination time for 96 h. When the light source was turned off, the concentrations of the three aldehydes decreased, indicating that light was at the origin of the creation of these species, however, substantial amounts did further react under dark conditions. This was not the case for acetone, the concentration of which practically did not change in the absence of light (Fig. 4). It should be reminded here that prior to GC/MS analysis, samples were filtered in order to remove small particles, some of them visually detected in solution after irradiation, in order to protect the GC column. Since no new reaction products were detected by GC/MS under dark conditions in the filtered samples, it may be concluded that consumption of the three aldehydes resulted in the formation of higher molecular weight products, which were removed from the samples by filtration.

3.3. UV/vis spectra

UV/vis spectra obtained from (unfiltered) samples collected in the course of the experiment are shown in Fig. 5a. It is observed that during the first few hours under irradiation, two bands appeared at about 235 and 275 nm. After prolonged irradiation times, a third band, centered at about 370 nm, appeared in the spectrum (traces d–g). The “tail” of the latter band in the visible region is responsible for the yellow color of the solution, which was seen by bare eye after about 20 h of illumination. As shown in Fig. 5b, the intensity of the 370-nm band increased with irradiation time, while the intensity of the 275-nm band varied with time in a manner which is qualitatively similar to that of the evolution of aldehydes detected by GC/MS (Fig. 4). It is of interest to note that when the UV lamps were turned off and the solution was left in the dark, the intensities of peaks at 235 and 275 nm did not significantly change (Fig. 5a). In contrast, the intensity of the 370-nm band continued to increase, indicating that reaction products, which are responsible for its appearance, can be formed even in the dark. Comparison with results of GC/MS experiments (Fig. 4) shows that the development of the 370-nm band in the absence of light can be related to consumption of aldehydes and formation of higher molecular weight products.

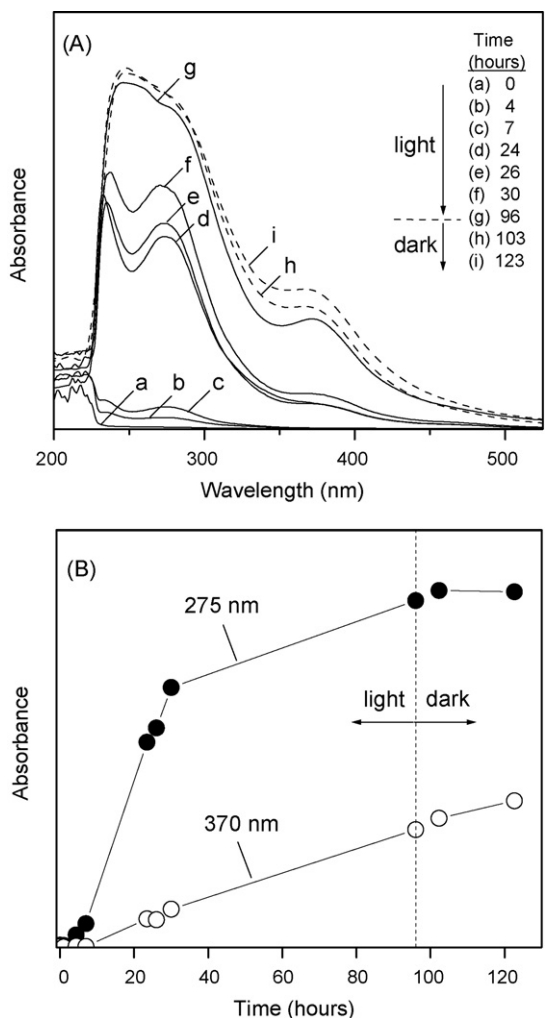


Fig. 5. (a) Variation of the absorption spectrum of the solution in the anode compartment during irradiation and in the dark; (b) variation of the absorbance with time at two characteristic wavelengths.

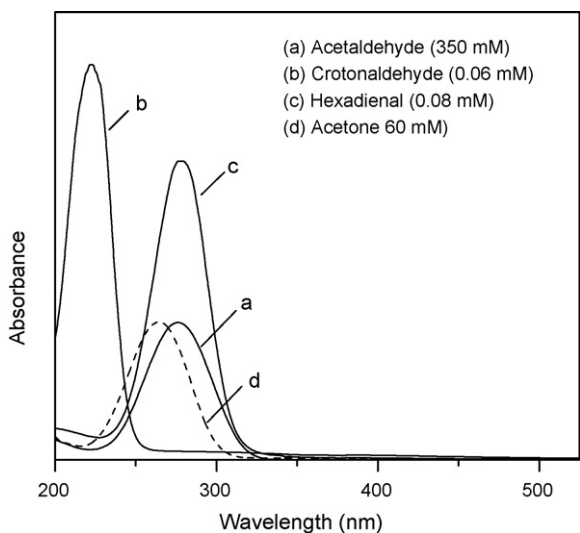


Fig. 6. Absorption spectra of some reagents corresponding to the substances detected by GC-MS.

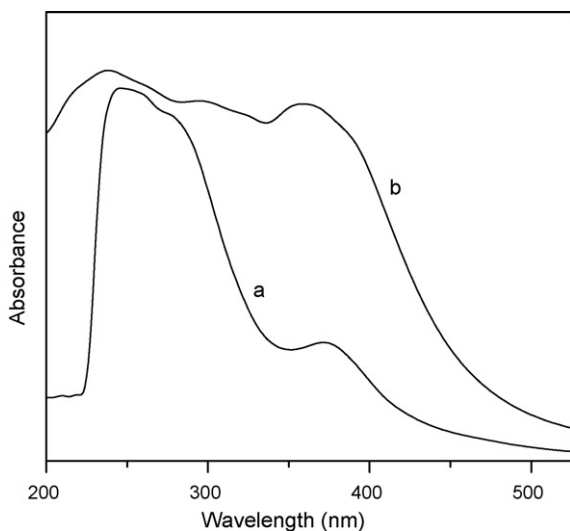


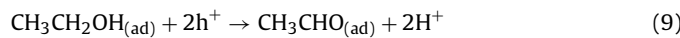
Fig. 7. Absorption spectrum of photoelectrochemically treated solution containing: (a) ethanol (20%v.) irradiated for 96 h; and (b) acetaldehyde (3.3%v.) irradiated for 24 h.

Fig. 6 shows UV/vis spectra obtained from alkaline, aqueous ethanol (20%v.) solutions containing small amounts of pure reagents corresponding to the compounds detected by GC/MS. In all cases, alkaline 20%v. ethanol solution was used as reference. In comparison with the spectra of Fig. 5a, it is concluded that the spectra of mixtures of acetaldehyde, crotonaldehyde, hexadienal and acetone can very well model the spectra of Fig. 5a, excluding the band at 370 nm. As will be discussed below, results presented in Figs. 4 and 5 can be explained by considering that crotonaldehyde, hexadienal and higher molecular weight products are formed via partial oxidation of ethanol toward acetaldehyde and subsequent aldol condensation reactions. In order to test this hypothesis, an experiment was conducted, in which ethanol was replaced by acetaldehyde reagent (3.3% by volume), under otherwise identical conditions. It was found that irradiation of the sample in the presence of the TiO_2 photocatalyst resulted in a relatively rapid development of the yellowish color and the formation of small particulate matter in solution, similar to that observed with ethanol. Fig. 7 shows the UV/vis spectrum obtained by irradiation of the alkaline–acetaldehyde–water solution for 24 h (trace b), in comparison to that obtained from the alkaline ethanol–water solution after 96 h (trace a). It is observed that photocatalytic treatment of the acetaldehyde-containing solution resulted in the development of similar but more intense bands, compared to the ethanol-containing solution, at significantly shorter irradiation times (24 h versus 96 h), especially at wavelengths above 350 nm. Results of Fig. 7 provide evidence that acetaldehyde produced by photo-induced oxidation of ethanol is the precursor of crotonaldehyde and hexadienal detected by GC/MS (Fig. 4) and of higher molecular weight products that are responsible for the appearance of the 370-nm band and for the yellow color of the solution. An additional experiment has been conducted with the use of the acetaldehyde-containing solution under dark conditions. It was observed that the yellowish color of the solution could be observed even in the absence of UV irradiation, although much less intense, indicating that aldol condensation reactions involving acetaldehyde proceed under the catalytic action of NaOH.

4. Discussion

4.1. Production of acetaldehyde by photocatalytic oxidation of ethanol

Results presented in Fig. 4 show that acetaldehyde appears in solution immediately after illumination, indicating that (i) ethanol is quickly photocatalytically oxidized toward acetaldehyde, and (ii) at least part of the produced acetaldehyde is weakly held on the photocatalyst surface and desorbs into the solution. This is in agreement with results of previous studies related to photocatalytic oxidation of ethanol in the liquid phase [11] or in the gas phase [15–19] and can be explained as follows: Ethanol adsorbs on the TiO_2 surface on at least two types of sites with different adsorption strength [17,19,20]: a chemisorbed Ti-bound ethoxide species and a molecularly adsorbed hydrogen-bonded species. Bandgap illumination of the ethanol-covered TiO_2 surface results in immediate formation of acetaldehyde, which is generally agreed to be the result of the first oxidation step [17–21]. The following elementary reaction steps can be considered:



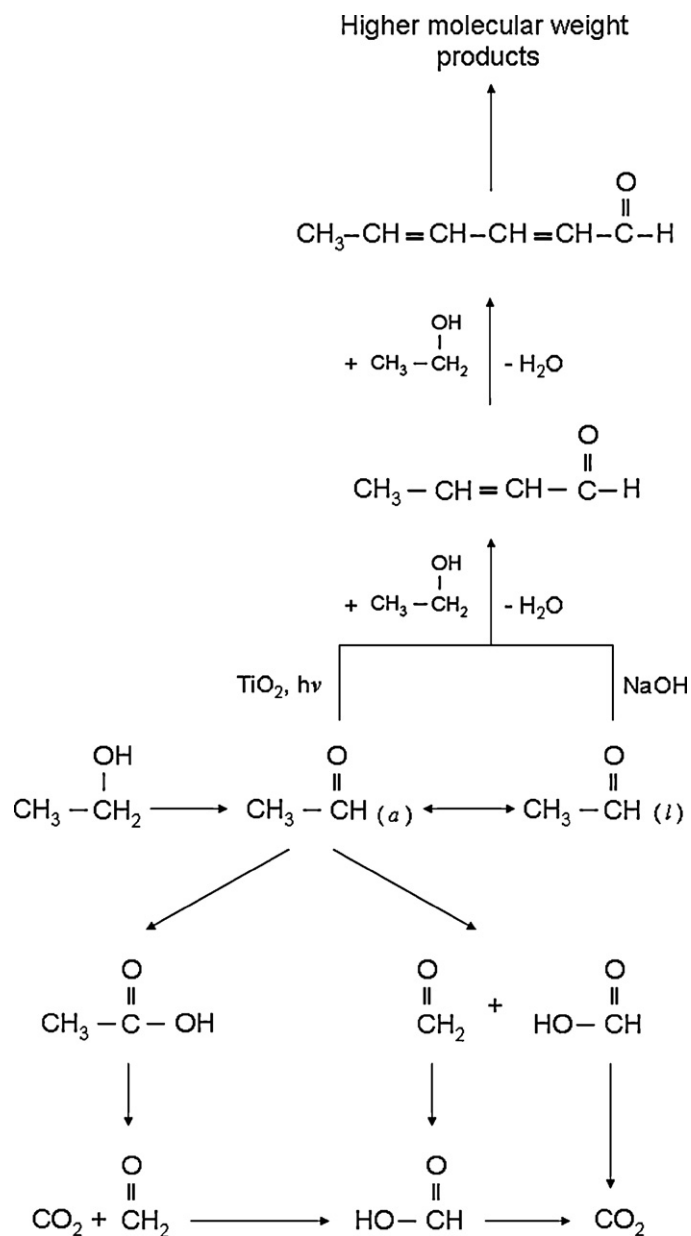
In reactions (9) and (10), subscripts “ad” and “l” refer to adsorbed and liquid-phase species, respectively. Weakly adsorbed ethanol yields acetaldehyde molecules which readily desorb from the photocatalyst surface, whereas strongly bound acetaldehyde is formed on the other ethanol adsorption site.

4.2. The fate of photo-produced acetaldehyde

The fate of photocatalytically produced acetaldehyde and the reaction pathway towards final products seems to strongly depend on the experimental conditions employed. Two general schemes can be considered: (i) photocatalytic oxidation of acetaldehyde to intermediate oxidation products and, eventually, to CO_2 ; (ii) oligomerization of acetaldehyde toward compounds of higher molecular weight via aldol condensation reactions. Both reaction pathways are shown in Scheme 1. The extent to which these pathways take place depends on several factors, including (1) photocatalyst formulation used (bare versus platinized TiO_2), (2) solution pH (natural versus basic), and (3) availability of oxygen (aerated versus deaerated solution, including oxygen mass transfer limitations).

4.2.1. Oxidation of acetaldehyde towards CO_2

Acetaldehyde formed by partial oxidation of ethanol may be photocatalytically oxidized toward CO_2 [21,22] via the two different reaction pathways shown in the lower part of Scheme 1 [17]. Reaction intermediates that have been identified in previous studies include acetic acid [17,22], formaldehyde [15,16], formic acid and methyl formate [15]. These species quickly react on illuminated TiO_2 and do not desorb in significant quantities at room temperature. As a result, they are present at low concentrations and cannot be easily detected. It may be noted here that in most studies performed in the gas phase, acetaldehyde is detected in the gas phase, indicating that the rate of its formation is higher than that of its subsequent oxidation to CO_2 . In fact, the slow reaction step has been proposed to be oxidation of acetaldehyde to acetic acid or formic



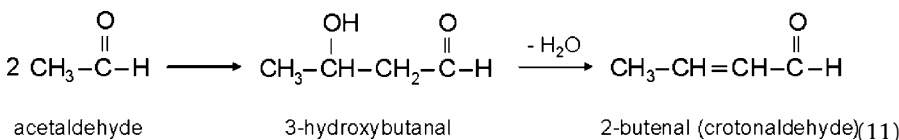
Scheme 1. Possible reaction pathways of acetaldehyde produced during photocatalytic treatment of alkaline solutions of ethanol over irradiated TiO_2 . Lower part: photocatalytic mineralization to CO_2 ; Upper part: oligomerization via aldol condensation reactions on the photocatalyst surface and in solution.

acid, while both the latter compounds can be rapidly oxidized to CO_2 [16].

It should be noted here that no CO_2 was detected in the gas phase under the present reaction conditions (use of alkaline solutions) under either Ar or air flow (Fig. 3). This is in contrast to what is observed during photocatalytic treatment of ethanol solutions at natural pH, which is known to result in progressive oxidation of ethanol to CO_2 both in the presence [23–26] and in the absence [10,27–29] of oxygen. The absence of CO_2 in the gas phase in the present experiments can be attributed to the well known ability of alkaline solutions to absorb significant amounts of carbon dioxide. Thus, evolution of CO_2 in the gas-phase would be expected to occur only after saturation of the solution with CO_2 , which, obviously, required much longer irradiation times than those used in the present experiments.

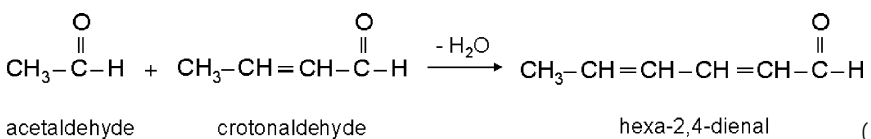
4.2.2. Aldol condensation of acetaldehyde

In addition to photocatalytic oxidation of acetaldehyde to CO_2 , and depending on the experimental conditions employed, a fraction of acetaldehyde may follow a different reaction pathway toward the formation of compounds of higher molecular weight via aldol condensation reactions that may take place on the photocatalyst surface and in solution (see upper part of Scheme 1). In aldol reactions, the conjugate base of an aldehyde (or ketone) adds to the carbonyl group of another aldehyde (or ketone) to give a new β -hydroxy aldehyde or ketone product. When this is followed by loss of a water molecule to form an α,β -unsaturated carbonyl compound, the reaction is called aldol condensation. For acetaldehyde, the initial aldol product is 3-hydroxybutanal, which may then dehydrate to give crotonaldehyde:



The aldol condensation of acetaldehyde is catalyzed by hydroxide ion (usually sodium hydroxide). This was presently verified in a separate experiment conducted in the dark. The alkaline environment in the above reactor then facilitates aldol condensation. The reaction may be also catalyzed by metal oxide catalysts, including TiO_2 , which offer the necessary acid or base sites. Idriss and Barteau [30] investigated reactions of acetaldehyde on TiO_2 (001) single crystal and provided evidence that self condensation of acetaldehyde to crotonaldehyde (11) is governed by surface oxygen anions (base sites). It was also shown that the reaction takes place more readily on oxidized TiO_2 , which contains more surface oxygen anions, whereas reduced surfaces promote the formation of butane via reductive coupling reaction [30]. Aldol condensation of acetaldehyde toward crotonaldehyde has been reported to occur under dark oxidation conditions over SrTiO_3 [31]. However, UV-irradiation of the SrTiO_3 photocatalyst resulted in the formation of CO_2 and partially oxidized species [31]. Obviously, the primary photocatalytic function in the case of a PFC running on ethanol is the production of sufficient quantity of acetaldehyde, which is the precursor for aldol condensation products.

Further aldolization of crotonaldehyde with acetaldehyde may result in the formation of hexa-2,4-dienal (12) which, in turn, can be aldolized toward C_8 and higher molecular weight compounds [32].



Compounds with more complicated structures can be produced via condensation of aldehydes on TiO_2 surface followed by cyclization [33], and/or by the addition reaction of adsorbed species (e.g., $-\text{CH}_2\text{CHO}$) to α,β unsaturated bonds toward branched, long-chain molecules that are held strongly on the TiO_2 surface [32]. It has been reported that Degussa P-25 has a much higher tendency to form longer chains, compared to other TiO_2 materials, because it has a higher concentration of acid sites and, therefore, a higher concentration of adsorbed acetaldehyde [32].

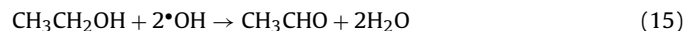
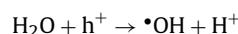
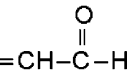
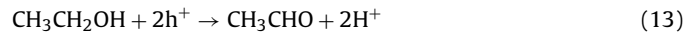
4.2.3. Formation of acetone

In addition to aldehydes discussed above, the photocatalytic reaction also resulted in the production of small but measurable amounts of acetone in solution (Fig. 4). As discussed in a previous study [11], acetone can be produced by interaction of acetaldehyde (or other reaction intermediates) with reactive radicals (such as

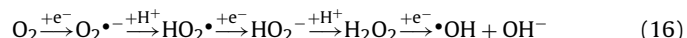
$\cdot\text{CH}_3$) formed via oxidation of organic species by photogenerated holes.

4.3. Why do aldol condensation reactions predominate under short-circuit conditions?

It is well known that photocatalytic oxidation reactions proceed by utilizing the high oxidation potential of photogenerated holes, which attack organic compounds either directly (13) or indirectly ((14)–(15)), via intermediate formation of hydroxyl radicals:

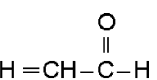


It is understood that reactions ((13)–(15)) are included in the overall scheme or reaction (1). Photogenerated electrons may migrate to the semiconductor surface and reduce chemisorbed O_2 to generate superoxide radical ($\text{O}_2\cdot^-$), which may then further react to form hydroperoxy radical ($\text{HO}_2\cdot$), hydrogen peroxide (H_2O_2) and hydroxyl radical ($\cdot\text{OH}$) [34–38]:



The so formed oxygen species are strong oxidants and can also attack organic compounds adsorbed on the photocatalyst surface and lead to their degradation [38–40].

Based on the above, it may be suggested that when the cell runs under open circuit conditions (anode and cathode not electrically connected), both photogenerated holes ((13)–(15)) and electrons (16) may contribute to the generation of



reactive species ($\cdot\text{OH}$, $\text{O}_2\cdot^-$, $\text{HO}_2\cdot$, H_2O_2) which, in turn, are responsible for the oxidation of ethanol and reaction intermediates toward CO_2 . However, under PFC operation (short-circuit conditions), electrons travel through the external circuit to the cathode electrode, where, in the presence of oxygen, they reduce O_2 according to reaction (4). Thus, under these conditions, only the oxidizing power of holes is utilized for oxidation reactions. In that case, it may be suggested that the oxidative power of the holes alone is not sufficient to efficiently oxidize all products of ethanol degradation and leaves space for aldol condensation reactions to occur.

4.4. The role of platinum

Another parameter, which seems to strongly affect the reaction pathway, is related to whether Pt is in intimate contact with TiO_2

photocatalyst, or not. In particular, when powdered Pt/TiO₂ photocatalysts are used for photocatalytic treatment of ethanol, this leads to its complete oxidation to CO₂ [23–26], even under unaerated conditions [10,27–29]. In the presence of oxygen, Pt-doping of TiO₂ results in an increase of the rates of alcohol conversion and CO₂ production [24–26]. Most important, platinization of TiO₂ determines to a large extent the distribution of reaction intermediates and products. This has been clearly shown by Chen et al. [23], who found that the concentration of acetaldehyde under conditions of photocatalytic oxidation of ethanol in aqueous slurries was 130 times higher on TiO₂ than on Pt/TiO₂. No aldol condensation has been observed in such cases. The same is true for acetaldehyde [10] and other compounds dealt with in the present study. However, when Pt is in another compartment (PFC mode) or when Pt is simply spatially isolated from TiO₂, aldol condensation reactions are favored against photooxidation. This can be understood in a way similar to that described above (Section 4.3). In addition, in dispersed Pt/TiO₂ catalysts, platinum crystallites (a) adsorb oxygen and supply it efficiently to the TiO₂ photocatalyst, and (b) may act as a conventional thermal oxidation catalyst. In this case, the role of Pt is to enhance the rate of ethanol oxidation by accelerating the oxygen reduction process, which is the rate-limiting step of oxidation reactions [23,41].

4.5. Ways of promoting mineralization of ethanol and suppressing aldol condensation reactions during PFC operation

The above data suggest that in order to achieve maximum benefit from a PFC it is necessary to design a reactor, which favors complete mineralization of the fuel. Obviously, this can be achieved under reaction conditions where acetaldehyde formed by partial oxidation of ethanol is quickly further oxidized toward CO₂, and aldol condensation reactions that may occur on the photocatalyst surface and in solution (Scheme 1) are suppressed. Ideally, for maximum PFC efficiency, this should be done in the absence of oxygen, i.e., by utilizing only water molecules as oxidants, so that photogenerated electrons could be solely used to produce electricity and not to reduce oxygen [16]. However, under the present experimental conditions, it seems that the presence of oxygen in the anode compartment is necessary in order to accelerate oxidation of acetaldehyde to CO₂ (lower part of Scheme 1) versus aldol condensation reactions (upper part of Scheme 1). In this case, oxygen mass transfer limitations are the first obstacles to overcome. Indeed, as already said, when the experiment was run under continuous air bubbling into the anode compartment, aldol condensation reactions were dramatically decreased. This is probably because reaction intermediates (mainly acetaldehyde) are quickly oxidized by oxygen on the photocatalyst surface and do not have the chance to participate in aldol condensation reactions.

Another factor that seems to affect the reaction pathway is the initial concentration of ethanol in solution, which may influence the relative population of adsorbed species on the photocatalyst surface. Indeed, no aldol condensation products were detected in cases where the concentration of the fuel was substantially smaller than the standard concentration used in this work, i.e. 20%. As seen in Fig. 2, almost 70% of the maximum current was obtained with only 1%v. alcohol, under the present experimental conditions. An optimized reactor should then run on an optimum combination of the quantity of the photocatalyst and the concentration of the fuel. The importance of reactor design in the functioning of PFC has been also treated in the works of Kaneko and co-workers [1–2].

Another parameter that should be taken into account is related to the solution pH, which can affect both the rate of mineralization of ethanol to CO₂ and the extent of aldol condensation reactions. It has been reported that CO₂ is produced immediately after illumination when ethanol photooxidation takes place

in acidic photocatalyst slurries, but the mineralization process can be substantially retarded in alkaline solutions [23]. As discussed above, aldol condensation reactions are also favored in alkaline solutions, especially in the presence of NaOH. Therefore, variation of solution pH and/or the use of a different electrolyte may have a beneficial effect in the overall cell performance. However, we observed that decrease of pH resulted in dramatic current drop. This is due to the fact that lack of OH[–] groups limits hole scavenging and favors electron-hole recombination, i.e., it acts against cell efficiency. Furthermore, in acidic pH it was observed that Degussa P25 detached itself from the FTO electrodes. Therefore, cell optimization will necessitate a delicate balance between all these opposing factors.

5. Conclusions

Alcohol was photocatalytically oxidized in a photoelectrochemical cell (PhotoFuelCell). Ethanol “burning” was accompanied by current flow in the external circuit. Current flow is affected by the process of oxidation and reaction pathway and it can be impeded by aldol condensation reactions. The first step in ethanol oxidation is production of acetaldehyde. Further oxidation towards complete mineralization is the desired process. However, when the relative rate of aldehyde formation is too high, aldol condensation leads to formation of relatively high molecular-weight species, which retard the mineralization process. In possible future applications of PhotoFuelCells, it will be necessary to either increase the rate of ethanol oxidation (mineralization) reaction under unaerated conditions or to avoid mass-transfer limitations and assure oxygen supply under aerated conditions. The concentration of photodegradable substance in solution must not be higher than that, which the photocatalyst can oxidize.

Acknowledgements

This work is supported by a project funded by E.ON AG as part of the E.ON International Research Initiative. Responsibility for the content of this publication lies with the authors.

References

- [1] M. Kaneko, J. Nemoto, H. Ueno, N. Gokan, K. Ohnuki, M. Horikawa, R. Saito, T. Shibata, *Electrochem. Commun.* 8 (2006) 336.
- [2] H. Ueno, J. Nemoto, K. Ohnuki, M. Horikawa, M. Hoshino, M. Kaneko, *J. Appl. Electrochem.* 39 (2009) 1897.
- [3] M. Kaneko, H. Ueno, R. Saito, S. Yamaguchi, Y. Fujii, J. Nemoto, *Appl. Catal. B* 91 (2009) 254.
- [4] T. Ohno, S. Izumi, K. Fujihara, Y. Masaki, M. Matsumura, *J. Phys. Chem. B* 104 (2000) 6801.
- [5] P.P. Kamat, *J. Phys. Chem. C* 111 (2007) 2834.
- [6] M. Antoniadou, P. Lianos, *J. Photochem. Photobiol. A* 24 (2009) 69.
- [7] M. Antoniadou, P. Lianos, *Catal. Today* 144 (2009) 166.
- [8] M. Antoniadou, D.I. Kondarides, D. Labou, S. Neophytides, P. Lianos, *Sol. Energy Mater. Sol. Cells* 94 (2010) 592.
- [9] T. Sakata, T. Kawai, *Chem. Phys. Lett.* 80 (1981) 341.
- [10] A. Patsoura, D.I. Kondarides, X.E. Verykios, *Catal. Today* 124 (2007) 94.
- [11] M. Antoniadou, D.I. Kondarides, P. Lianos, *Catal. Lett.* 129 (2009) 344.
- [12] S. Ito, P. Chen, P. Comte, M.K. Nazeeruddin, P. Liska, P. Pechy, M. Gratzel, *Prog. Photovolt.: Res. Appl.* 15 (2007) 603.
- [13] M. Antoniadou, E. Stathatos, N. Boukos, A. Stefopoulos, J. Kallitsis, F.C. Krebs, P. Lianos, *Nanotechnology* 20 (2009), Art.No. 495201.
- [14] M. Antoniadou, P. Bouras, N. Strataki, P. Lianos, *Int. J. Hydrogen Energy* 33 (2008) 5045.
- [15] M.R. Nimlos, E.J. Wolfrum, M.L. Brewer, J.A. Fennell, G. Binter, *Environ. Sci. Technol.* 30 (1996) 3102.
- [16] M.L. Sauer, D.F. Ollis, *J. Catal.* 158 (1996) 570.
- [17] D.S. Muggli, J.T. McCue, J.L. Falconer, *J. Catal.* 173 (1998) 470.
- [18] D.S. Muggli, K.H. Lowery, J.L. Falconer, *J. Catal.* 180 (1998) 111.
- [19] D.S. Muggli, J.L. Falconer, *J. Catal.* 175 (1998) 213.
- [20] S.-J. Hwang, D. Raftery, *Catal. Today* 49 (1999) 353.
- [21] A.V. Vorontsov, G.B. Baraqnnik, O.I. Snegurenko, E.N. Savinov, V.N. Parmon, *Kinet. Catal.* 38 (1997) 84.

- [22] I. Sopyan, M. Watanabe, S. Murasawa, K. Hashimoto, A. Fujishima, J. Photochem. Photobiol. A 98 (1996) 79.
- [23] J. Chen, D.F. Ollis, W.H. Rulkens, H. Bruning, Water Res. 33 (1999) 661.
- [24] J. Chen, D.F. Ollis, W.H. Rulkens, H. Bruning, Water Res. 33 (1999) 1173.
- [25] A.V. Vorontsov, V.P. Dubovitskaya, J. Catal. 221 (2004) 102.
- [26] J.C. Kennedy, A.K. Datye, J. Catal. 179 (1998) 375.
- [27] B. Ohtani, M. Kakimoto, S. Nishimoto, T. Kagiya, J. Photochem. Photobiol. A 70 (1993) 265.
- [28] D.I. Kondarides, V.M. Daskalaki, A. Patsoura, X.E. Verykios, Catal. Lett. 122 (2008) 26.
- [29] V.M. Daskalaki, D.I. Kondarides, Catal. Today 144 (2009) 75.
- [30] H. Idriss, M.A. Barreau, Catal. Lett. 40 (1996) 147.
- [31] C.-A. Chang, B. Ray, D.K. Paul, D. Demydov, K.J. Klabunde, J. Mol. Catal. A 281 (2008) 99.
- [32] S. Luo, J.L. Falconer, Catal. Lett. 57 (1999) 89.
- [33] C. Huang, D.H. Chen, K. Li, Chem. Eng. Commun. 190 (2003) 373.
- [34] M.V. Rao, K. Rajeshwar, V.R. Pal Verneker, J. DuBow, J. Phys. Chem. 84 (1980) 1987.
- [35] H. Gerischer, A. Heller, J. Phys. Chem. 95 (1991) 5261.
- [36] T. Wu, G. Liu, J. Zhao, H. Hidaka, N. Serpone, J. Phys. Chem. B 103 (1999) 4862.
- [37] T. Wu, T. Lin, J. Zhao, H. Hidaka, N. Serpone, Environ. Sci. Technol. 33 (1999) 1379.
- [38] M. Styliidi, D.I. Kondarides, X.E. Verykios, Appl. Catal. B 47 (2004) 189.
- [39] O. Legrini, E. Oliveros, A.M. Braun, Chem. Rev. 93 (1993) 671.
- [40] M.R. Hoffmann, S.T. Martin, W. Choi, D.W. Bahnemann, Chem. Rev. 95 (1995) 69.
- [41] D. Hufschmidt, D. Bahnemann, J.J. Testa, C.A. Emilio, M.I. Litter, J. Photochem. Photobiol. A 148 (2002) 223.